

ELECTRICAL AND OPTICAL STUDIES IN $\text{Ge}_{100-x}\text{S}_x$ CHALCOGENIDE THIN FILMS

H.S. METWALLY

Physics Department, Faculty of Education, Ain Shams University
Roxy, Cairo, Egypt

(Received December 8, 2000; revised version April 10, 2001)

Thin films of $\text{Ge}_{100-x}\text{S}_x$ with different values of x are deposited on quartz substrates by a conventional thermal evaporation technique. The electrical conductivity of these films was measured. The experiments reveal that the electronic conduction is strongly composition dependent and is thermally activated with a single activation energy for $x > 40$. A variable range hopping conduction mechanism seems to dominate when $x = 16$ and 27. The optical absorption of the films is investigated using spectrophotometric measurements of the transmittance and reflectance in the wavelength range 200–3000 nm. All the studied compositions obey the Tauc relation concerning the non-direct transitions. The optical energy gap E_g value increases with the increase in chalcogen content x . The Urbach parameter E_0 decreases from 310 meV to 149 meV as x increases from 16 to 70.

PACS numbers: 73.61.Jc, 78.66.Jg

1. Introduction

Germanium based chalcogenide glasses receive great attention due to their potential use in various solid state devices [1–5]. They are an interesting and unique class of amorphous materials. They have a widely different lattice structure in crystalline and non-crystalline form. This is contrary to other vitreous semiconductors, which have similar short-range order in the two states [6]. Glass formation and structure of Ge–S system have been studied and reported by several authors [7–9]. Some workers [10–16] have investigated electrical and optical properties of such system.

This paper presents a systematic investigation of some electrical and optical properties of five compositions of the Ge–S amorphous system, which have not been widely investigated so far.

2. Experimental

$\text{Ge}_{100-x}\text{S}_x$ compositions ($x = 16, 27, 52, 65,$ and 70) in bulk form were prepared by the conventional melt quenching technique [17]. Proper quantities of high purity elements (99.999%) were mixed together and sealed in evacuated silica ampoules (10^{-3} Pa). The mixture was heated at 1273 K for 24 h in an oscillatory furnace. The temperature was raised in steps in order to reduce the vapor pressure of the constituent components. The molten composition was quenched in cold water. It was confirmed by X-ray diffraction that the ingots thus obtained were amorphous. Films of different thickness were prepared at room temperature by thermal evaporation in a vacuum of 10^{-3} Pa under the same evaporation conditions using a high vacuum unit (Edwards E306A) on well cleaned quartz substrates of the suitable dimensions. The composition of the films was determined using the energy dispersive X-ray spectrometer (EDS) analysis. The film thickness was estimated by Tolansky's method [18], using multiple-beam Fizeau fringes. The film thickness was ≈ 1500 nm. The rate of evaporation was ≈ 0.6 nm/s. Substrate temperature was ≈ 300 K.

Electrical measurements were made in a vacuum of ≈ 0.1 Pa in a specially designed cryostat. The film resistance was measured with a programmable electrometer (Keithley 617) in coplanar configuration using Al electrodes. The reflection and transmission measurements were carried out using (UV-3101PC) spectrophotometer in the range 200–3000 nm at room temperature.

3. Results and discussion

The X-ray diffraction patterns obtained for various $\text{Ge}_{100-x}\text{S}_x$ ($x = 16, 27, 52, 65,$ and 70) films illustrate that the samples under investigation have an amorphous nature.

Preliminary thermoelectric power (Seebeck coefficient) measurements showed that our samples exhibit *p*-type electrical conduction, which agrees with the previously reported [2, 19].

Although there is not a definite critical composition which separates the activation type conduction (linear relation between $\log \sigma$ and T^{-1}) from the variable range hopping (VRH) conduction (linear relation between $\log \sigma$ and $T^{-1/4}$), the latter conduction mechanism seems to dominate in the composition range where x is smaller than 40 for $\text{Ge}_{100-x}\text{S}_x$ films. The variation of the dc conductivity (σ) with reciprocal temperature ($1/T$) for five compositions of $\text{Ge}_{100-x}\text{S}_x$ ($x = 16, 27, 52, 65,$ and 70) films is shown in Fig. 1a. The plot of $\log \sigma$ vs. $1/T$ gives a straight line obeying the following exponential relation:

$$\sigma = \sigma_0 \exp(-E_a/kT), \quad (1)$$

where σ_0 is the pre-exponential factor, E_a is the thermal activation energy and k is the Boltzmann constant. In general, the conductivity was increased either by increasing temperature or by increasing Ge content. Table summarizes the results obtained for the used samples. The σ_0 values calculated for the compositions with $x > 40$ are within the range 4.8×10^4 – 4.7×10^6 ($\Omega \text{ cm}$) $^{-1}$. Following Mott and

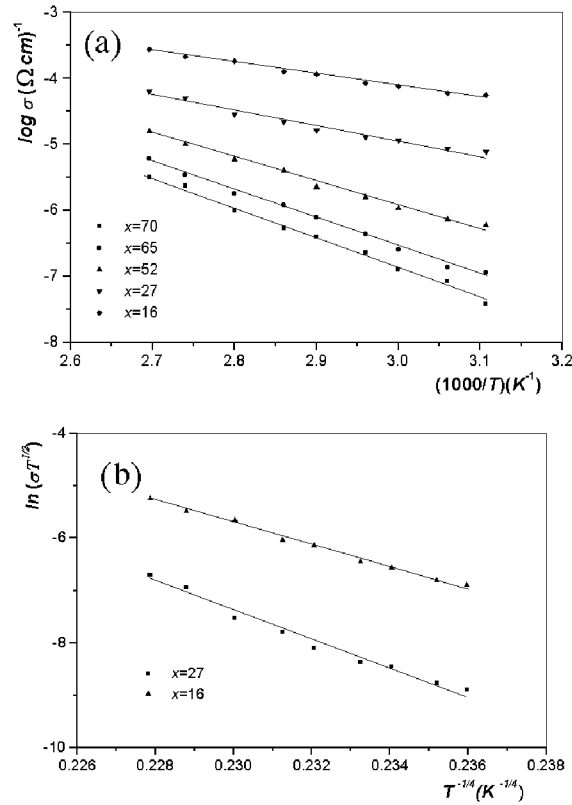


Fig. 1. (a) Temperature dependence of dc conductivity for $\text{Ge}_{100-x}\text{S}_x$ films with different compositions. (b) $\ln(\sigma T^{1/2})$ versus $T^{-1/4}$ plot for $\text{Ge}_{100-x}\text{S}_x$ films with $x = 16$ and 27.

Davis [20] these high values of σ_0 indicate that conduction takes place in the extended states. However, the smallest values of σ_0 for the compositions with $x = 16$ and 27 suggest that conduction is due to carriers excited into the localized states at the band edge [21]. The $\ln(\sigma T^{1/2})$ can be plotted linearly against $T^{-1/4}$ for films of $x = 16$ and 27 as shown in Fig. 1b, indicating that the transport is due to VRH of the charge carriers in the localized states near the Fermi level, and is characterized by Mott's VRH relation [22]. The density of localized states around the Fermi level, $N(E_F)$, is obtained from $\ln(\sigma T^{1/2})$ vs. $T^{-1/4}$ plot by assuming the decay length of the localized states to be 1 nm. For $x = 16$ and 27 $N(E_F)$ is found to be 1.1×10^{17} and $3.9 \times 10^{16} \text{ eV}^{-1} \text{ cm}^{-3}$, respectively, which is in a reasonable agreement with the results of Ref. [11].

The absorption coefficient $\alpha(\omega)$ is calculated according to the relation

$$\alpha(\omega) = (1/d) \ln[(1 - R)^2/T_0], \quad (2)$$

where d is the film thickness, R is the reflectance, T_0 is the transmittance and ω is the angular frequency. The optical absorption curves of different compositions

TABLE

Measured values of thermal activation energy E_a , pre-exponential factor σ_0 , optical energy gap E_g , the band tailing parameter B , and the Urbach parameter E_0 for different compositions.

Composition	E_a [eV]	σ_0 [$(\Omega \text{ cm})^{-1}$]	E_g [eV]	B [$(\text{eV cm})^{-1}$]	E_0 [meV]
Ge ₈₄ S ₁₆	0.34	11.18	0.88	9.89×10^5	310
Ge ₇₃ S ₂₇	0.45	62.8	0.96	4.1×10^5	296
Ge ₄₈ S ₅₂	0.69	4.95×10^4	1.5	3.38×10^5	239
Ge ₃₅ S ₆₅	0.85	9.85×10^5	2.29	2.55×10^5	165
Ge ₃₀ S ₇₀	0.91	4.92×10^6	2.59	1.8×10^5	149

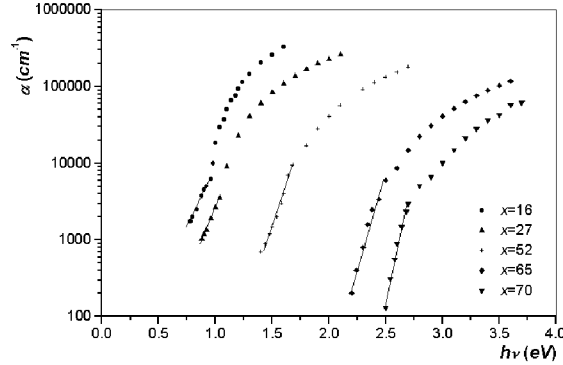


Fig. 2. The change of absorption coefficient α with x . The lines drawn on curves indicate the range of $h\nu$ used to calculate E_0 .

are shown in Fig. 2. As shown in this figure, the absorption curves shift to higher values as the Ge content increases i.e. sulfur content (x) decreases, similar results are shown by others [11, 23].

In amorphous as in crystalline materials some useful information can be deduced from absorption edge measurements, even though in such materials the edge is less sharp than in crystals. For many amorphous materials an exponential dependence of the absorption coefficient α on photon energy $h\nu$ is found to hold over wide range and takes the form [24, 25]:

$$\alpha(\omega) = \alpha_0 \exp(h\nu/E_0), \quad (3)$$

where α_0 is a constant, h is Planck's constant and E_0 is an energy, which is interpreted as the width of the tail of the localized states in the normally forbidden band gap. These are associated with the disorder of amorphous systems. This relation was first proposed by Urbach [24] to describe the absorption edge in alkali halide crystals at high absorption levels. The calculated values of E_0 are listed in Table. Values of E_0 are found to decrease from 310 to 149 meV as the chalcogen content x increases. The increase in E_0 with the increase in Ge content indicates an increase in disorder in Ge-S system. Similar phenomena are also seen for amorphous Ge [26].

To define the optical gap, E_g , Tauc et al. [27] proposed the following expression for the non-direct transition:

$$(\alpha h\nu) = B(h\nu - E_g)^2, \quad (4)$$

where $h\nu$ is the incident photon energy and B is the band tailing parameter. E_g is then calculated by a linear extrapolation of the $(\alpha h\nu)^{1/2}$ vs. $h\nu$ to the energy axis as shown in Fig. 3. The energy gap E_g for different compositions estimated in this work is in a good agreement with the previously reported one [12, 28]. The physical basis of the Tauc expression is the assumption of parabolic energy bands, an energy-independent momentum matrix element and a relaxation of momentum conservation. It is clear from Table that the estimated values of B for different compositions are of the right order of magnitude when comparing with those obtained for different amorphous semiconductors [21]. Figure 4 shows the optical gap E_g as a function of chalcogen content x . From this figure one can observe that the energy gap E_g increases with the increase in chalcogen content x . This result is in accordance with that previously reported by Shimizu et al. [11].

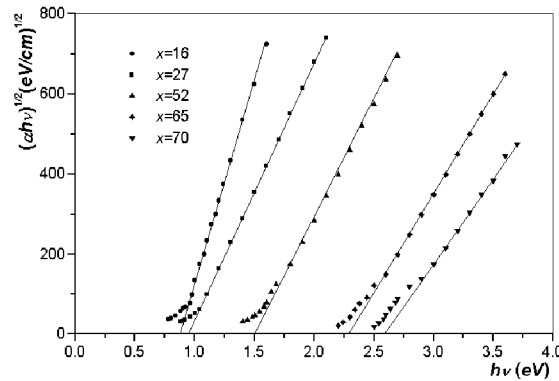


Fig. 3. Dependence of $(\alpha h\nu)^{1/2}$ on the photon energy $h\nu$ for different x values.

Cody et al. [29] found that $E_0(T1, X1)$ and $E_g(T1, X1)$ are proportional to each other, where $T1$ and $X1$ represent the thermal and structural disorder, respectively. The relation between E_0 and E_g is investigated through this study as shown in Fig. 5. A similar linearity as described by Cody is found. This favours our indication about the direct relation between the increase in structural disorder, represented by E_0 , and the decrease in optical gap as the chalcogen content decreases.

Germanium chalcogenide glasses can be described as small chemically ordered clusters embedded in a continuous network as proposed by Phillips [30]. In $\text{Ge}_x\text{S}_{1-x}$ glass, some of these clusters are $(\text{S})_n$ chains, $\text{Ge}(\text{S}_{1/2})_4$ corner sharing tetrahedral, and $\text{Ge}_2(\text{S}_{1/2})_6$ ethane-like structural units which dominate $\text{Ge}_x\text{S}_{1-x}$ alloys near $x = 0, 0.33$, and 0.4 , respectively [2]. In the S-rich region the first two types of clusters would dominate. Ge atoms are fourfold coordinated and S atoms are twofold coordinated. Almost all bonds are Ge-S_x for $x = 2$, but there exist Ge-S and S-S bonds in the glass with $x > 2$ and Ge-S and Ge-Ge bonds in that

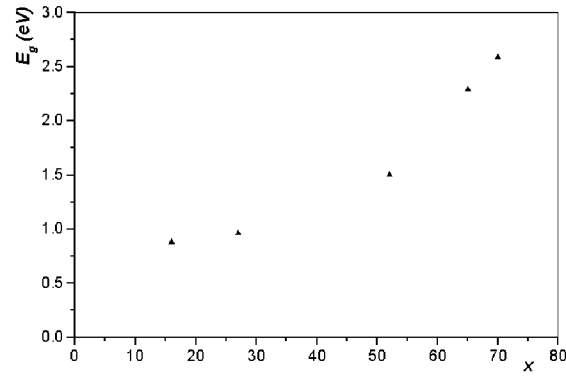


Fig. 4. The optical gap E_g as a function of chalcogen content.

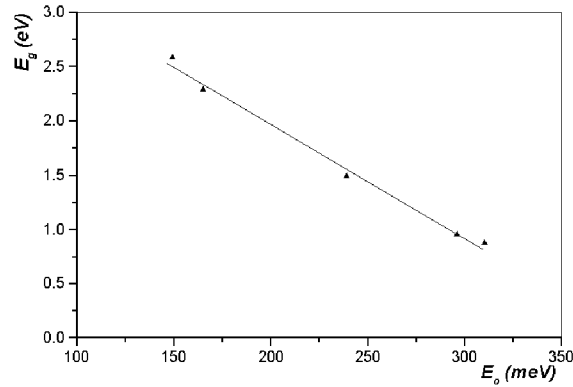


Fig. 5. Linear variation of the Tauc gap E_g and the Urbach parameter E_0 with respect to changes in x .

with $x < 2$. In the glass with $x < 2$, bond breaking will take place more likely at Ge–Ge bond (37.6 kcal/mole) which is weaker than Ge–S bond (55.52 kcal/mole). Assuming that most of incorporated chalcogen atoms are twofold coordinated, there are following several possibilities for the origin of the decrease in $N(E_F)$ and increase in E_g by the addition of chalcogen atoms:

1. Chalcogen atoms introduce the lone-pair character to the valence band, making the effective electron correlation energy U in the dangling bond states negative. As a result, dangling bonds become charged ones D^+ and D^- .
2. Chalcogen atom works as a terminator to Ge dangling bond just as hydrogen or possibly oxygen does [31, 32].
3. Introduction of twofold coordinated chalcogen atoms makes tetrahedrally bonded structure of Ge flexible, so that the density of dangling bonds is reduced [23].

4. Conclusions

In this work, we have studied the change in some electrical and optical properties of $\text{Ge}_{100-x}\text{S}_x$ thin films as a function of the chalcogen content x . Analysis of the experimental results reveals that the electronic conduction is composition dependent and thermally activated for $x > 40$. A variable range hopping conduction mechanism seems to dominate when $x = 16$ and 27 . From absorption coefficient studies, all compositions under test show a non-direct transition according to the Tauc relation. The optical energy gap E_g value increases with the increase in chalcogen content x , while the Urbach parameter E_0 decreases. It could be concluded that the structural disorder, represented by E_0 , increases as the chalcogen content decreases which is accompanied by the decrease in the optical energy gap.

References

- [1] K.C. Tai, W.R. Sinclair, R.G. Vadimsky, J.M. Moran, *J. Vac. Sci. Technol.* **16**, 1977 (1979).
- [2] K.L. Bhatia, D.P. Gosain, G. Parthasarathy, E.S.R. Gopal, *Phys. Rev. B* **34**, 8786 (1986).
- [3] M. Sudha, A. Girridhar, A.K. Singh, *J. Non-Cryst. Solids* **103**, 179 (1988).
- [4] H. Yang, S. Min, J. Lu, F. Zhang, *J. Non-Cryst. Solids* **112**, 176 (1989).
- [5] T.C. Arnoldussen, C.A. Menezes, Y. Nakagawa, R.H. Bube, *Phys. Rev. B* **9**, 3377 (1974).
- [6] K.L. Bhatia, G. Parthasarathy, E.S.R. Gopal, *J. Phys. Chem. Solids* **45**, 1189 (1984).
- [7] I.M. Migolinels, M.Yu. Sichka, *Sov. J. Glass Phys.* **5**, 256 (1979).
- [8] A. Feltz, M. Ppohle, H. Steil, G. Herms, *J. Non-Cryst. Solids* **69**, 271 (1985).
- [9] M. Ppohle, A. Feltz, G. Herms, *J. Non-Cryst. Solids* **69**, 283 (1985).
- [10] I. Watanabe, T. Maeda, T. Shimizu, *J. Non-Cryst. Solids* **37**, 335 (1980).
- [11] T. Shimizu, I. Watanabe, M. Kumeda, M. Ishikawa, *J. Non-Cryst. Solids* **35&36**, 895 (1980).
- [12] T. Shimizu, M. Kumeda I. Watanabe, Y. Nakagaki, *Solid State Commun.* **27**, 223 (1978).
- [13] R. Mathur, A. Kumar, *Solid State Commun.* **61**, 785 (1987).
- [14] E.A. Zhilinskaya, V.N. Lazukin, N.Kh. Valeev, A.K. Oblasov, *J. Non-Cryst. Solids* **124**, 48 (1990).
- [15] M. Fadel, A.A. Nijim, H.T. El-Shair, *Vacuum* **46**, 1275 (1995).
- [16] F. Abd-El-Salam, M. Fadel, K. Sedeek, *Vacuum* **45**, 835 (1994).
- [17] M. Fadel, A.A. Nijim, H.S. Metwally, M.A. Affifi, *Appl. Phys. A* **54**, 288 (1992).
- [18] S. Tolansky, *Multiple-Beam Interferometry of Surface and Films*, Oxford University Press, London 1948.
- [19] V.K. Bhatnagar, K.L. Bhatia, D.P. Gosain, V.K. Jain, *J. Non-Cryst. Solids* **92**, 302 (1987).
- [20] N.F. Mott, *Philos. Mag.* **22**, 7 (1970).

- [21] N.F. Mott, E.A. Davis, *Electronic Processes in Non-Crystalline Materials*, Clarendon Press, Oxford 1979.
- [22] H. Kori, K. Cotoch, H. Sahata, *J. Non-Cryst. Solids* **183**, 122 (1995).
- [23] D. Minkov, E. Vateva, E. Skordeva, D. Arsova, M. Nikiforova, *J. Non-Cryst. Solids* **90**, 481 (1987).
- [24] R. Urbach, *Phys. Rev.* **92**, 1324 (1953).
- [25] S.K.J. Al-Ani, C.A. Hogarth, *J. Mater. Sci.* **20**, 661 (1985).
- [26] S.K. O'Leary, S. Zukotynski, J.M. Perz, *J. Non-Cryst. Solids* **210**, 249 (1997).
- [27] J. Tauc, R. Grigorovici, A. Vancu, *Phys. Status Solidi* **15**, 627 (1966).
- [28] L. Tichy, A. Triska, C. Barta, H. Ticha, M. Frumar, *Philos. Mag. B* **46**, 365 (1982).
- [29] G.D. Cody, T. Tiedje, B. Abeles, B. Brooks, Y. Goldstein, *Phys. Rev. Lett.* **47**, 1480 (1981).
- [30] C. Phillips, *J. Non-Cryst. Solids* **55**, 179 (1983).
- [31] G.A.N. Connell, J.R. Pawlik, *Phys. Rev. B* **13**, 787 (1976).
- [32] D.K. Pandia, S.K. Barthwal, K.L. Chpra, *Phys. Status Solidi A* **32**, 489 (1975).

